NASA Technical Memorandum 88963

Experimental Evaluation of a Translating Nozzle Sidewall Radial Turbine

(NASA-TM-88963) EXPERIMENTAL EVALUATION OF A TRANSLATING NOZZLE SIDEWALL RADIAL TURBINE (NASA) 22 p CSCL 21E

N87-17701

Unclas
G3/07 43336

Richard J. Roelke
Lewis Research Center
Cleveland, Ohio

and

Casimir Rogo
Teledyne CAE
Toledo, Ohio

Prepared for the
69th Symposium of the AGARD Propulsion and Energetics Panel
on Technology for Advanced Aero Engine Components
Paris, France, May 4–8, 1987

NASA

EXPERIMENTAL EVALUATION OF A TRANSLATING NOZZLE SIDEWALL RADIAL TURBINE

Richard J. Roelke
Research Engineer
NASA Lewis Research Center
21000 Brookpark Road
Cleveland, OH 44135

and

Casimir Rogo
Project Manager
Aerodynamic Components
Teledyne CAE
1330 Laskey Road
Toledo, OH 43612

SUMMARY

An experimental performance evaluation was made of two moveable sidewall variable area radial turbines. The turbine designs were representative of the gas generator turbine of a variable flow capacity rotorcraft engine. The first turbine was an uncooled design while the second turbine had a cooled nozzle but an uncooled rotor. The design, fabrication and testing were carried out by Teledyne CAE under a series of government contracts. Performance measurements were taken over a turbine flow range of 2:1 in the Contractor's warm (121 °C) air facility. The cooled nozzle turbine was evaluated both with and without coolant flow.

The test results showed that the moveable nozzle wall is a viable and efficient means to effectively control the flow capacity of a radial turbine. Peak efficiencies of the second turbine with and without nozzle coolant were 86.5 and 88 percent respectively. These values are comparable to pivoting vane variable geometry turbines; however, the decrease in efficiency as the flow was varied from the design value was much less for the moveable wall turbine. The measured turbine performance over the entire flow range was within one point of the estimated turbine performance used in a previously conducted variable flow capacity engine analysis which showed significant fuel savings. Several design improvements were identified which should increase the turbine efficiency one or more points. These design improvements include reduced leakage losses and relocating the vane coolant ejection holes to reduce mainstream disturbance.

E-3419

INTRODUCTION

A major programmatic thrust at the NASA Lewis Research Center is to improve the performance and fuel economy of small (0.9 to 2.3 kg/sec airflow size) gas turbine engines. Significant performance improvements of this engine class have been made over the years with optimized engine cycles, improved small component performance and the incorporation of higher temperature materials and cooling technology. Further fuel savings may be made (Ref. 1) by utilizing ceramics in the hot section, allowing higher temperatures and reduced coolant flows, and developing nonconventional cycles such as regenerative engines. These approaches increase the engine's thermal efficiency. Another approach to reducing the total fuel burned is to improve the part-power fuel consumption. This is particularly important for an engine that operates over a wide power range as in a rotorcraft application. Here the objective of a reduction of total fuel consumption can be effectively made by a variable flow capacity engine.

Typically, engines are designed to be most efficient at a selected operating condition (or power level), for a given application, and increased fuel consumption is accepted at other power levels. As is well known, the increased fuel consumption is due to higher losses as the engine components operate off-design. In the variable flow capacity engine, the components are operated at constant conditions during the entire flight and the engine power is modulated by changing engine airflow. This is accomplished by operating the turbomachinery at their design values of speed, pressure ratio and turbine inlet temperature and utilizing variable geometry for airflow management. The variable capacity engine was included in an Army study (Ref. 2), where it was concluded that the lack of data on variable geometry made the evaluation of the cycle difficult and that research efforts should focus on the critical variable geometry loss/leakage issues in the engine components. Later Army sponsored studies (Refs. 3 and 4), provided in-depth analyses of the losses and performance of variable nozzle area gas generator radial turbines. These studies showed fuel savings for the variable flow cycle compared to a simple cycle, if the aerodynamic penalties of the variable geometry could be kept low.

The latter two studies focused on the variable geometry gas generator turbine since this was one of the riskiest components in the engine and the one about which very little information existed. For this turbine, two methods were considered to vary the nozzle area. One was by translating the nozzle sidewall and the second was by pivoting the vanes or the trailing edge portion of the vanes. The results indicated that the translating sidewall method had the same or lower losses than the pivoting vanes, but lacked substantiating data. An experimental program was recommended to obtain data for the translating sidewall turbine.

A series of Army funded - NASA managed contracts were awarded to Teledyne CAE to obtain turbine performance data on the translating sidewall concept. Initially, a variety of moving sidewall configurations were tested to establish a data base and identify the one or two concepts with the best performance. An existing uncooled turbine design was used for those tests. Information gained from the test program was then incorporated into the turbine design of Ref. 4 and a second research turbine built. The purpose of the second turbine was to determine the effect of nozzle vane coolant flows and improved vane leakage control on turbine performance.

The testing was done at the Contractor's site. Tests were conducted with air at a temperature of 121 °C and a pressure of 164 kPa. Overall stage performance and selected flow surveys were taken. This paper summarizes the results of the program.

TURBINE DESIGN

A cross section of a conceptual variable flow capacity engine is shown in Fig. 1. The engine has a two-stage compression system, a reverse flow combustor, a radial gas generator turbine, and an axial flow power turbine with a forward output shaft. All the turbomachinery in the engine has variable geometry. The compressors have variable inlet guide vanes and translating sidewall diffusers, while both turbines have variable area nozzles. There is no variable geometry in the combustor. A single mechanical linkage simultaneously actuates all variable geometry components with a single control.

Several cycle and mechanical variations of this engine were studied and analyzed for a defined rotorcraft mission (Refs. 3 and 4). A design life of 4000 hr with projected year 1990 materials was specified. Both cooled and uncooled rotors were considered for the gas generator turbine. Design parameters of one of the selected engines are listed in Table I. Comparison of the performance of this engine with a comparable technology simple cycle showed a seven percent fuel savings for the variable cycle engine. Additional study details may be found in Ref. 4.

The engine studies formed the basis of the variable geometry turbine designs. Two turbine designs were recommended. One design had an inlet temperature of 1370 °C with a cooled nozzle and rotor, while the other turbine had an inlet temperature of 1205 °C, a cooled nozzle and an uncooled rotor. The lower temperature design was selected for the test program. The design engine airflow, i.e., the flow corresponding to the nominal setting of the variable geometry, and the airflow range were selected based on the vehicle power demands and an optimization study made to minimize the total fuel burned for the mission. Results indicated a flow variation of 2:1 was required with the design airflow set at 78 percent of the maximum flow. The two methods considered for turbine flow control, the pivoting vane and moving sidewall nozzles, are shown in Fig. 2. The variable geometry losses associated with the pivoting vanes are leakage flows between the vanes and sidewalls and incidence changes as the vanes are rotated. The losses associated with the moving sidewall are leakage flows on the telescoping side of the nozzle plus sudden expansion and contraction losses as the sidewall is moved.

First Test Turbine

As mentioned earlier, the initial turbine utilized in the test program was an existing design of Teledyne CAE. The turbine had been designed some years earlier, but the design conditions were sufficiently close to those specified for this program. A variation of the design was also used in a test program to evaluate the pivoting vane turbine and could therefore serve as a reference against which to compare the moving sidewall turbine. To adapt the turbine for use in this program the machine was scaled up (to a rotor diameter of 355.6 mm) to match facility and Reynolds number requirements and the nozzle hardware was redesigned to accept various kinds of moving sidewalls. The nominal design conditions for this turbine are listed in Table II and the meridional flow path is shown in Fig. 3.

The test objective for this turbine was to evaluate several stator configurations. Typical geometries are shown in Fig. 4. Both straight and contoured sidewalls as well as various vaneless space geometries were tested. Figure 4(a) shows a sudden expansion or dump into the vaneless space as the nozzle is closed down. The next configuration, Fig. 4(b), depicts a diffusing ramp in the vaneless space that is actuated by and follows the moving wall. The intent is to reduce sudden expansion losses. The next illustration, Fig. 4(c), shows a converging vaneless space where the flow is accelerated smoothly as the nozzle is opened to its maximum area. However, this configuration still results in a sudden expansion at closed down areas. In Fig. 4(d), the vaneless space wall travels with the nozzle wall and the flow dump occurs in the rotor inducer where there are lower relative velocities than in the vaneless space.

In each configuration, one of the nozzle sidewalls was always in a fixed position and aligned flush with the inlet and vaneless space walls. The opposite sidewall was then positioned to either increase or decrease the flow area from the nominal setting. At the nominal setting, both walls are aligned flush with the rotor inducer. All nozzle vanes of the first turbine were solid and no coolant flow was simulated.

Tests with this turbine were also conducted with variable geometry at the rotor exit. This consisted of rings that were inserted into the flow just downstream of the rotor to control the rotor reaction as the stator was closed down. The stage efficiency decreased for all rotor exit ring tests and will not be reported on further in this paper. Additional design and configuration details are included in Ref. 5.

Second Test Turbine

The second research turbine was essentially the design executed in Ref. 4 with some modifications made based on the results of the first turbine tests. Design parameters are listed in Table III. The flow path of the turbine, as taken from an engine layout, is shown in Fig. 5. The use of current cooling technology and year 1990 materials required coolant in the nozzle vanes, sidewalls, and rotor shroud, plus a small amount to purge the rotor backface cavity. No rotor coolant was required. All coolant flows except the shroud flow was simulated in the test turbine. The nozzle was designed with straight sidewalls and a converging vaneless space. The test turbine was built so either the hub or shroud walls could be moved. Photographs of the two rotors and nozzle vanes are shown in Fig. 6.

Vane Seals

During the design and test phases of the program, careful attention was given to the leakage flow around the nozzle vanes. The gap between the sidewall cutout and the vane profile was nominally 0.4 mm. Tests were run with this gap open, completely sealed with a rubberized sealant and finally with a metal wiper seal. The seals are shown in Fig. 7. A cross section of the "L" shaped seal is shown in section B-B. Based on pressure measurements, it appeared that the leakage flow followed a path as shown in the figure which caused significant losses. In the first turbine, Fig. 7(a), only a portion of the vane clearance gap was sealed with the wiper seal. The region is shown by the cross hatched area in the figure. The application of the wiper seal to this small area was very effective; however, the seal was extended to most of the vane perimeter for the second turbine. The effectiveness of the seals is discussed later in this paper.

APPARATUS AND TEST PROCEDURE

The research turbines were evaluated in a test facility at Teledyne CAE. A cross section of the test apparatus is shown in Fig. 8. Compressed air at a nominal pressure of 164 kPa was heated to about 121 °C and ducted to the inlet plenum of the turbine. Within the inlet plenum the flow passed through two screens to smooth the flow before entering the turbine. After leaving the turbine, the air was ducted to facility exhausters. The turbine pressure ratio was set by changing the exit pressure. Power was absorbed by a waterbrake which also served to control the speed. Between the turbine and waterbrake was an in-line torque meter which measured the shaft torque and rotational speed.

The instrumentation installed in the test rig is shown in Fig. 9. At station 1, about one-half vane chord upstream of the nozzle, measurements of total temperature, total pressure and wall static pressure were taken. At this same location, surveys of flow angle and pressure were taken from wall to wall to verify the flow uniformity at the turbine inlet. At station 2 were located wall static pressure taps and an angle/total pressure survey probe. The survey probe was used to measure from wall-to-wall axially and over a distance of one and one-half vane pitches circumferentially. Wall static pressures were measured on the inner and outer walls at stations 3 and 4. A radial survey probe for measuring angle, total pressure and total temperature was located at station 3. At station 4, twelve values each of total pressure and temperature were measured with fixed rakes. The coolant and mainstream flow rates were measured with calibrated flow orifices.

For each turbine configuration tested, the nozzle sidewalls were moved in increments (usually four) from full open to 50 percent closed by means of jack screws with a pneumatic assist. Stops were provided to repeat the nozzle area settings accurately as the nozzle configurations were changed. The nozzle sidewall position could also be set and/or measured with a depth gage through access holes in the nozzle assembly. The first turbine was set up so that at the flush wall condition the nozzle area was 80 percent of the maximum area, whereas it was 78 percent for the second turbine. The nozzle assembly of the second turbine used to simulate vane coolant flows is shown schematically in Fig. 10. The coolant entered a small plenum behind the hub sidewall and then flowed through a series of small holes into the mainstream to simulate vane and wall cooling. A small amount of coolant also entered the mainstream from the rotor backface plenum.

All testing with the first turbine was conducted at design speed and pressure ratio. For each nozzle configuration, stage performance data were taken over a range of flow areas. Based on the results of those tests, five geometries were selected for detail flow surveys at the nozzle and rotor exits. Testing with the second turbine was limited to fewer nozzle configurations but for expanded operating conditions. Data were taken at speeds of 60, 80, and 100 percent of design and for a range of pressure ratios above and below the design value. Data were also taken with and without nozzle coolant flows.

The turbine efficiency was calculated from both torque measurements and the turbine temperature drop. Measured values of tare torque (for bearing, seals and windage losses) were added to the shaft torque to get the total turbine torque. Comparison of the efficiencies calculated from the two methods, as well as mass averaged efficiency values from surveys, showed very good agreement. Torque derived efficiencies were intended to be the primary basis for performace comparisons but recurring mechanical problems with the waterbrake and torquemeter gave occasional erratic results. Therefore, most of the comparisons were made based on temperature derived efficiencies.

RESULTS AND DISCUSSION

This section presents a summary of the test results of the two research turbines and the impact of those results on the variable flow capacity engine. Over the span of seven years of this program much valuable research has been accomplished and information gathered. Therefore, of the voluminous amount of data, only the most salient results are presented here. A great deal of additional information is contained in Refs. 3 through 7.

First Research Turbine

The first turbine build was tested without any leakage control at the location where the vanes passed through the nozzle sidewall. The test build consisted of a moveable hubwall with a vaneless space dump, see for example Fig. 4(a). The resulting measured turbine efficiency is shown in Fig. 11 by the symbol labeled "no seal." The test was repeated first with the clearance gaps totally sealed with a rubber compound and then with the flexible metal wiper seal shown in Fig. 7(a). The turbine performance from both of these tests was the same and is indicated by the symbol labeled (1) in Fig. 11. The turbine air flow decreased 7.4 percent and the efficiency increased 2-1/2 points for the sealed vane tests when compared to the unsealed vane test. The wiper seal employed is typical of what could be used in an engine and was used for the remainder of the turbine tests.

A summary of the overall performance results with the first research turbine is given in Fig. 12. The peak efficiency ranged from 87 to 87.3 percent for the different turbine builds and occurred, as expected, with flush aligned nozzle walls. All of the nozzle configurations with the straight sidewalls performed similarly. The contoured nozzle configurations were definitely lower in performance and had different flow characteristics. The nozzle contouring was rather arbitrarily added to the straight wall design and its incorporation into the vane design was not individually optimized. This may explain its lower performance. There was very little difference in performance between moving the hub or shroud walls. At intermediate flow reductions (i.e., 65 percent of the maximum nozzle area), the moveable shroud wall builds performed slightly better than moveable hub wall builds, but the reverse was true at greater flow reductions. The change in efficiency from the peak value to the value at 50 percent nozzle flow area was approximately 2-1/2 points for the moving hub wall and 3-1/2 points for the moving shroud wall. The choice of which wall to move may be selected on the basis of mechanical actuation considerations.

Based primarily on results such as those shown in Fig. 12, two straightwall nozzle configurations with converging vaneless spaces were selected for detailed stator exit flow surveys. The pressure and flow angle measurements taken between two adjacent vanes are shown in Fig. 13. Surveys were taken for four nozzle areas with a moveable shroud wall and one nozzle area with a moveable hub. The rotor was installed and rotating during the surveys. The nozzle wall position is indicated on the figure. High pressure losses (Fig. 13(a)), occurred along the shroud as the nozzle shroud wall was moved into the flow stream indicating probable flow separation. A loss core was also measured near the hub side. This may have been due to air flowing in the vane clearance gap between the main channel flow and the plane of the wiper seal. Locating the wiper seal nearer to the mainstream, as shown in Fig. 14(b), should reduce this hub loss, however this seal change was not evaluated for either turbine. The dashed line in Fig. 13 represents the measured loss with the moveable hub wall. In this case, any recirculating clearance gap flow is shifted from the hub side to the shroud side. However, that by itself does not account for the large pressure loss measured near the shroud. Overall mass weighted pressure losses are listed in the figure.

The angle measurements (Fig. 13(b)), show that changes in flow direction occurred mostly over two-thirds of the channel on the shroud side. As the nozzle area was reduced, the flow angle measured from radial was increased, which is consistent with continuity considerations. The maximum change in flow angle as the nozzle area was changed occurred at 80 percent of the inducer width and equaled 10°.

Second Research Turbine

The effect of vane leakage flow on the performance of the second test turbine is shown in Fig. 15. These leakage tests were conducted in a similar manner to the first research turbine. Tests were run at design speed with the vane gap completely sealed and then with the wiper seals installed. Data were taken for a range of pressure ratios at two nozzle area settings, 78 (flush wall) and 100 percent of the maximum area. For the higher pressure ratios tested, the loss in efficiency was about one-fourth point for the flush walls and about one and one-fourth points for the maximum flow area. These losses are greater than those of the first turbine and may be due to the different pressure gradients around the redesigned vane profile.

The effect of nozzle coolant flow on turbine efficiency is shown in Fig. 16 for a stator with flush aligned walls operating at design speed and pressure ratio. A reference test was made with no coolant flow to either the nozzle or rotor backface cavity. The resulting efficiency is shown by a triangle. Data were also taken with a constant coolant flow of 1 percent to the backface cavity and for a nozzle coolant flow range of 0 to 6 percent. As can be seen, as the nozzle coolant flow was increased the turbine efficiency first increased and then decreased. At the design coolant flow of 5.6 percent, the efficiency was 1.6 points less than the reference value when all coolant flows were zero.

The nozzle coolant was then fixed at 5.6 percent of the mainstream flow as the nozzle flow area was varied. Since the wall position determined the primary flow, cooling was increased or decreased in direct proportion to the vane surface area exposed to the mainstream thus simulating an engine application. The results while operating the turbine at design speed and pressure ratio are summarized in Fig. 17.

All data in the figure were obtained with straight nozzle sidewalls, a converging vaneless space, and vane wiper seals. Both moveable hub and shroud wall geometries are included. The top curve is for a turbine without coolant flow and could represent a machine utilizing a ceramic nozzle assembly. The bottom curves are for 5.6 percent nozzle coolant flow and 1.0 percent rotor backface flow. The peak efficiencies for the cooled and uncooled turbines were 86.4 and 88.0 respectively. The moveable hub and shroud wall geometries performed similarly except for the cooled turbine at the 50 percent closed position. At that condition, the moveable hub turbine efficiency was 2.2 points higher than the moveable shroud turbine. This increased loss, with the moveable shroud, is probably due to the location of the flow disturbance caused by the coolant ejected into the clearance gap, see Fig. 10. This gap coolant enters the rotor hub region where there is low reaction and flow diffusion. A similar effect occurs with the moving hub wall but with a lower loss due to the higher reaction along the rotor shroud. It is felt that the efficiency levels shown in Fig. 17 can be increased by: 1) reducing the leakage loss by relocating the wiper seal as discussed earlier; and 2) redesigning the vane coolant circuit to locate the ejection holes in the mainstream for all wall positions. The latter improvement would apply only to the cooled turbine.

Comparison with Pivoted Vane Turbines

Shown in Fig. 18 is a comparison of the performance of the two moveable sidewall turbines with pivoting vane turbines. Many of the turbines compared had different design requirements and applications and so the comparison is made on a nondimensional basis. The moveable sidewall turbines used in these comparisons were the best performing configurations of the first and second test turbines. The Teledyne pivoting vane turbine, listed in the figure, was the design used for the first moveable wall turbine and therefore had the same rotor and vane profiles.

The two moveable wall turbines and the Teledyne pivoting vane turbine had peak efficiencies of generally the same level (not shown in the figure), but the moveable wall turbines maintained substantially higher efficiencies as the flow was varied. The efficiency difference would be even greater than shown if the pivoting vane turbine had realistic vane endwall clearances. During that test program, for each vane angle set, the nozzle sidewalls were drawn against the vanes to eliminate the clearance gap.

The moveable wall turbines also compared well against the two turbines of Refs. 8 and 9. Those two turbines were evaluated for reasons other than variable geometry. In each case, a series of integral machined nozzles were designed to match a single rotor. Each nozzle was uniquely designed for a given stagger angle and in some instances, the number of vanes was changed to obtain an optimum condition. Also, the integral nozzle assembly resulted in no leakage loss. If those turbines were true variable geometry designs, their efficiency loss would be expected to increase from that shown.

Comparison of Measured and Predicted Turbine Performance

The efficiency of the moveable sidewall turbine was estimated for use in the variable flow capacity engine cycle calculations of Ref. 4. It was arrived at by adding a leakage loss and a sudden contraction or expansion loss to a predicted radial turbine performance map. The change in efficiency from the design point is shown in Fig. 19 by a solid curve. The change in efficiency from the peak efficiency of the cooled moving hub wall turbine, taken from Fig. 17, is shown for comparison. The research turbine slightly exceeded the estimated performance for flows larger than design flow and was slightly lower at low flows. In general, the test results compare well with the estimate. A redesigned nozzle coolant circuit, as discussed earlier, should raise the efficiency level in the low flow range. The absolute level of turbine efficiency used in the engine cycle calculations was about one point higher than the experimental values. However, a further reduction in seal loss would raise the overall efficiency level of the moveable sidewall turbine. A further increase in turbine efficiency could be realized if ceramics were used in the nozzle reducing or eliminating the coolant flows.

A more recent cycle analysis of the variable flow capacity engine, utilizing the test results of this program, was made and is reported in Ref. 10. The approach differed from the earlier study, Ref. 4, in that the turbomachinery was not kept at constant conditions for the entire mission. Engine power was varied by a combination of RPM and variable geometry changes during the flight. The resulting fuel consumption was compared to the "best" 1984 engines and an advanced technology engine of the 1990's. The results indicated that the variable geometry engine had fuel savings of 26 percent compared to the best 1984 engine, and 11 to 14 percent compared to the 1990's engine in the 60 percent power range.

SUMMARY OF RESULTS

A performance evaluation was made of a moveable sidewall variable area radial turbine applicable to a variable flow capacity rotorcraft engine. The primary results of the investigation follow.

1. The moveable nozzle sidewall concept is a viable method to efficiently control the flow capacity of a radial turbine. The investigation quantified the performance of turbines with cooled and uncooled nozzles and the effect of variable geometry leakage flows.

2. Peak efficiencies at design speed and pressure ratio of 86.4 and 88 percent were measured for cooled and uncooled turbines respectively. The efficiency decrease from the peak value was about 5 points at 50 percent flow and 2-1/2 points at 100 percent flow for the best performing configurations.

3. The level of the turbine performance was one point or less over the entire flow range from the component estimate used in a variable flow capacity engine cycle which showed significant fuel savings. Several design improvements were identified which should increase the turbine efficiency one or more points.

4. The moveable wall and pivoting vane variable geometry concepts had about the same maximum efficiency, but the efficiency decreased significantly less as the flow was changed with the moveable wall.

5. The best performing turbine configuration had straight nozzle sidewalls and a converging vaneless space. Similar performance results were obtained with either the hub or shroud wall moveable except for the cooled nozzle configuration at 50 percent flow area. For that case, the moveable hub performed better.

6. A flexible metal wiper seal proved to be an effective means of controlling leakage flow around the nozzle vanes.

REFERENCES

1. Vanco, M.R.; Wintucky, W.T.; and Niedzwiecki, R.W.: An Overview of the Small Engine Component Technology (SECT) Studies. AIAA Paper 86-1542, June 1986.

2. Easterling, A.E.: A Comparative Study of Simple, Regenerative, and Variable Capacity Cycles for Gas Turbine Engines. USAAVRADCOM-TR-81-D-1, Oct. 1980.

3. Large, G.D.; and Meyer, L.J.: Cooled, Variable-Area Radial Turbine Program. NASA CR-165408, 1982.

4. Rogo, C.; and Holbrook, M.R.: Cooled Variable Nozzle Radial Turbine for Rotor-Craft Applications. (Teledyne-CAE-1759, Teledyne CAE; NASA Contract NAS3-22005) NASA CR-165397, 1981.

5. Rogo, C.; Hajek, T.; and Chen, A.G.: Variable Stator Radial Turbine. (Teledyne-CAE-1987, Teledyne CAE; NASA Contract NAS3-23163), NASA CR-174663, 1984.

6. Rogo, C.; Hajek, T.; and Roelke, R.: Aerodynamic Effects for Moveable Sidewall Nozzle Geometry and Rotor Exit Restriction on the Performace of a Radial Turbine. Advances in Aerospace Propulsion, SAE-P-131, SAE, 1983, pp. 71-81.

7. Rogo, C.: Variable Area Radial Turbine Fabrication and Test Program. (Teledyne-CAE-2231, Teledyne CAE; NASA Contract NAS3-23173) NASA CR-175091, 1986.

8. Kofskey, M.G.; and Wasserbauer, C.A.: Experimental Performance Evaluation of a Radial-Inflow Turbine Over a Range of Specific Speeds. NASA TN D-3742, 1966.

9. Kofskey, M.G.; and Nusbaum, W.J.: Effects of Specific Speed on Experimental Performance of a Radial Turbine. NASA TN D-6605, 1972.

10. Rogo, C.; and Benstein, E.H.: Variable Cycle Turboshaft Technology for Rotorcraft of the '90s. J. Propulsion Power, vol. 2, no. 1, Jan.-Feb. 1986, pp. 73-80.

TABLE I. - VARIABLE FLOW CAPACITY ENGINE CONDITION AT 71 m/s FLIGHT VELOCITY AND 82 PERCENT POWER

Inlet pressure, kPa	103.4
Inlet temperature, °C	17.2
Compressor pressure ratio	16
Compressor efficiency, percent	78.3
Combustor pressure drop, percent	3
Combustor efficiency, percent	99.5
GG turbine inlet temperature, °C	1205
GG turbine inlet pressure, kPa	1602.4
GG turbine efficiency, percent	88
Power turbine exit pressure, kPa	107.6
Power turbine exit temperature, °C	578
Power turbine efficiency, percent	88
Shaft power (82 percent of maximum), kW	515
Airflow, kg/s	1.63
Fuel consumption, kg/kW-hr	0.257

TABLE II. - FIRST RESEARCH TURBINE EQUIVALENT DESIGN CONDITION AT 80 PERCENT FLOW

Airflow, kg/s	1.28
Pressure ratio	4.50
Speed, rpm	16540
Specific work, kJ/kg	87.88
Work factor	0.93
Tip diameter, mm	355.6
Tip speed, m/s	306.7

TABLE I. - VARIABLE FLOW CAPACITY ENGINE CONDITION AT 71 m/s FLIGHT VELOCITY AND 82 PERCENT POWER

Inlet pressure, kPa	103.4
Inlet temperature, °C	17.2
Compressor pressure ratio	16
Compressor efficiency, percent	78.3
Combustor pressure drop, percent	3
Combustor efficiency, percent	99.5
GG turbine inlet temperature, °C	1205
GG turbine inlet pressure, kPa	1602.4
GG turbine efficiency, percent	88
Power turbine exit pressure, kPa	107.6
Power turbine exit temperature, °C	578
Power turbine efficiency, percent	88
Shaft power (82 percent of maximum), kW .	515
Airflow, kg/s	1.63
Fuel consumption, kg/kW-hr	0.257

TABLE II. - FIRST RESEARCH TURBINE EQUIVALENT DESIGN CONDITION AT 80 PERCENT FLOW

Airflow, kg/s	1.28
Pressure ratio	4.50
Speed, rpm	16540
Specific work, kJ/kg .	87.88
Work factor	0.93
Tip diameter, mm . . .	355.6
Tip speed, m/s	306.7

TABLE III. - SECOND RESEARCH TURBINE DESIGN CONDITIONS AT 78 PERCENT FLOW

	Engine	Equivalent (2x size)
Rotor inlet temperature, °C	1205	14.5
Inlet pressure, kPa	1602.4	101.4
Airflow, kg/s	1.77	1.44
Rotor speed, rpm	71000	15940
Tip diameter, mm	176.7	353.4
Tip speed, m/s	656.9	294.9
Pressure ratio	4.094	4.54
Specific work, kJ/kg	442.5	88.7
Total efficiency, percent	87.3	87.3
Work factor	1.03	1.03
Nozzle coolant, percent	5.6	5.6
Rotor backface coolant, percent	1.0	1.0

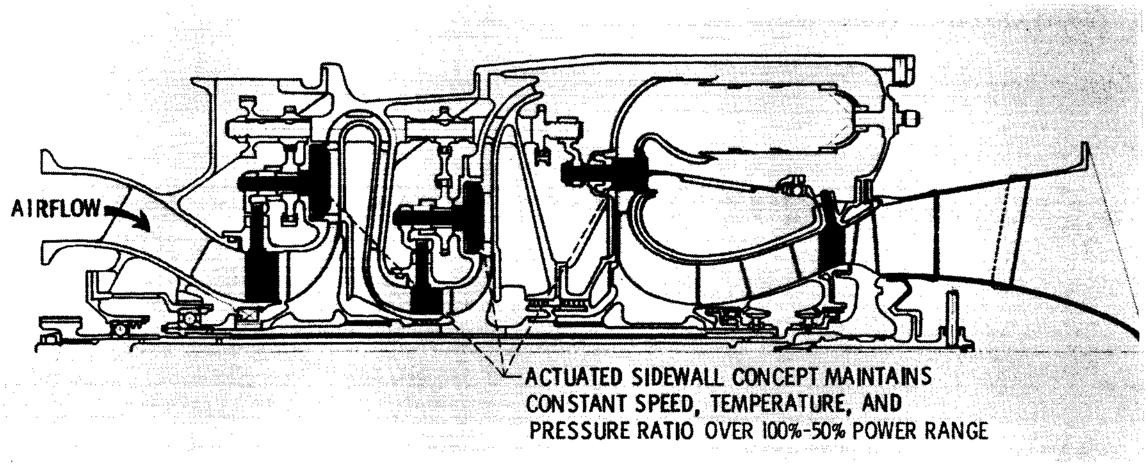

FIGURE 1. - CONCEPTUAL VARIABLE FLOW CAPACITY ENGINE.

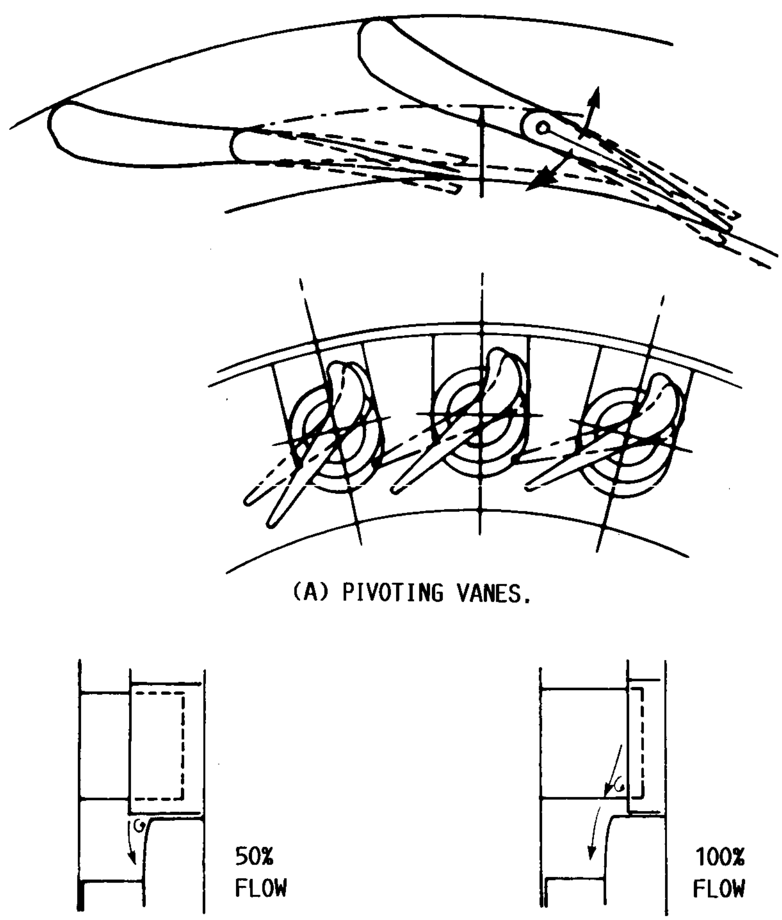

(A) PIVOTING VANES.

(B) MOVING SIDEWALLS.

FIGURE 2. - VARIABLE NOZZLE AREA CONCEPTS.

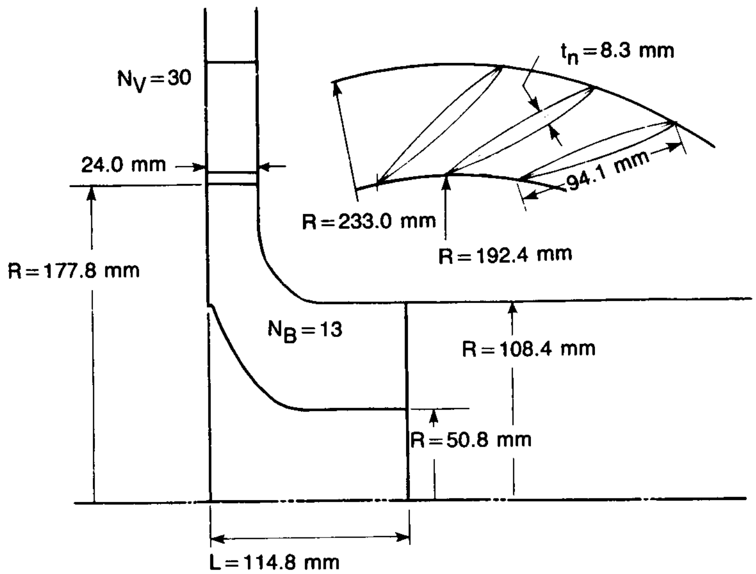

FIGURE 3. - FIRST RESEARCH TURBINE FLOWPATH.

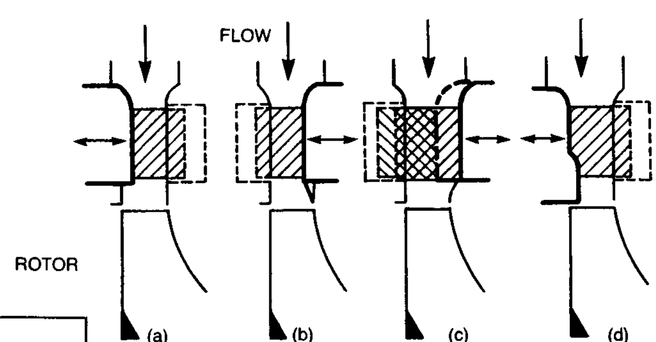

FEATURE	(a)	(b)	(c)	(d)
VANE WALLS WALL MOVED VANELESS SPACE	STRAIGHT HUB DUMP	STRAIGHT SHROUD DIFFUSER	STRAIGHT SHROUD CONVERGING	CONTOURED HUB LOW RADIUS DUMP

FIGURE 4. - TYPICAL CONFIGURATIONS TESTED.

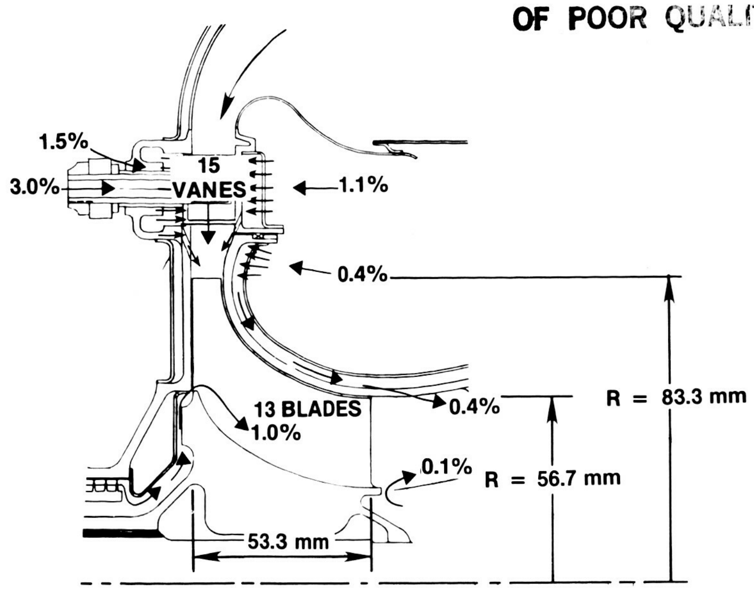

FIGURE 5. - SECOND RESEARCH TURBINE SHOWN IN ENGINE LAYOUT.

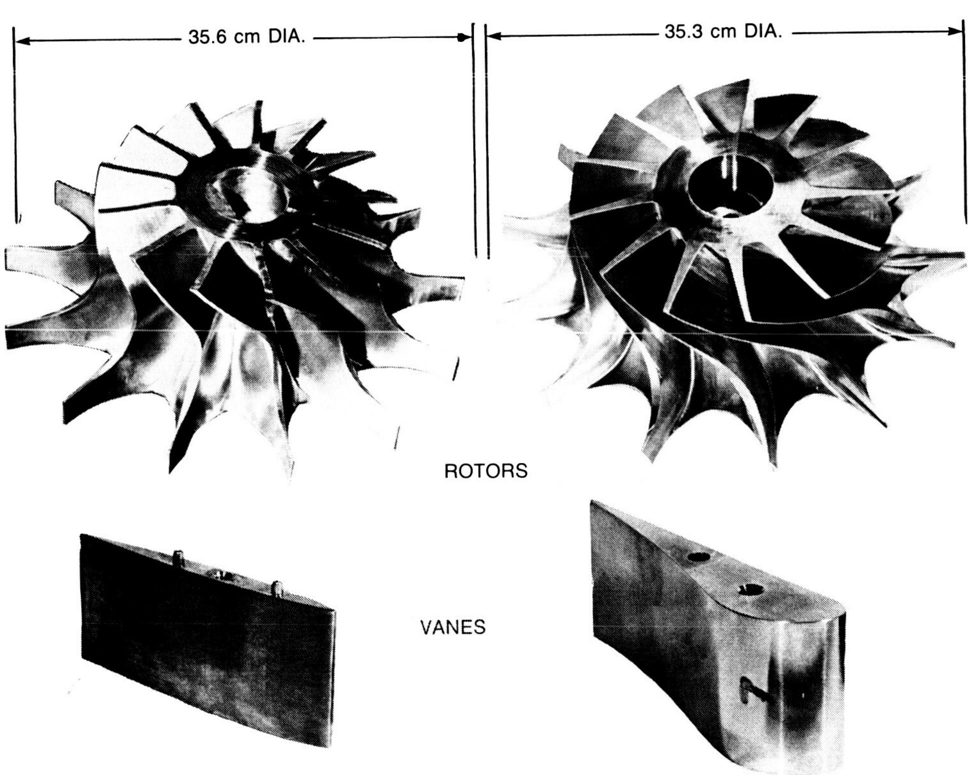

(A) FIRST TURBINE. (B) SECOND TURBINE.

FIGURE 6. - RESEARCH TURBINE BLADING.

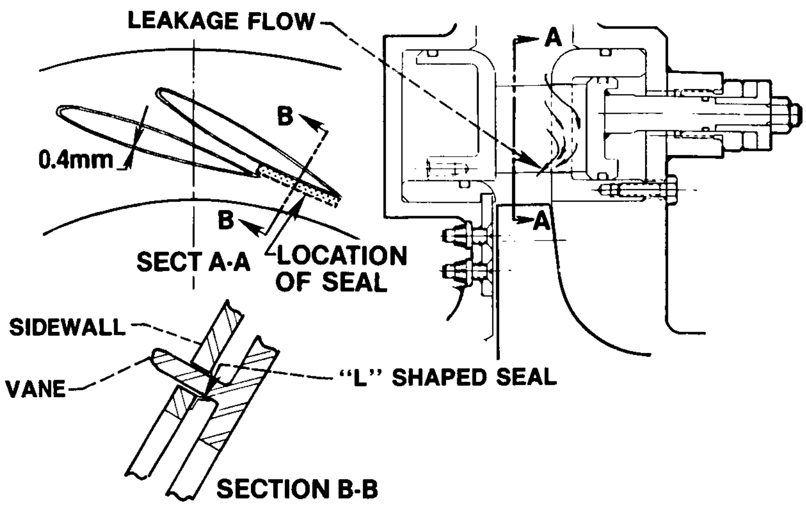

(A) FIRST TURBINE.

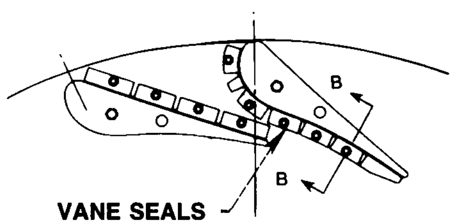

(B) SECOND TURBINE.

FIGURE 7. - VANE LEAKAGE CONTROL SEALS.

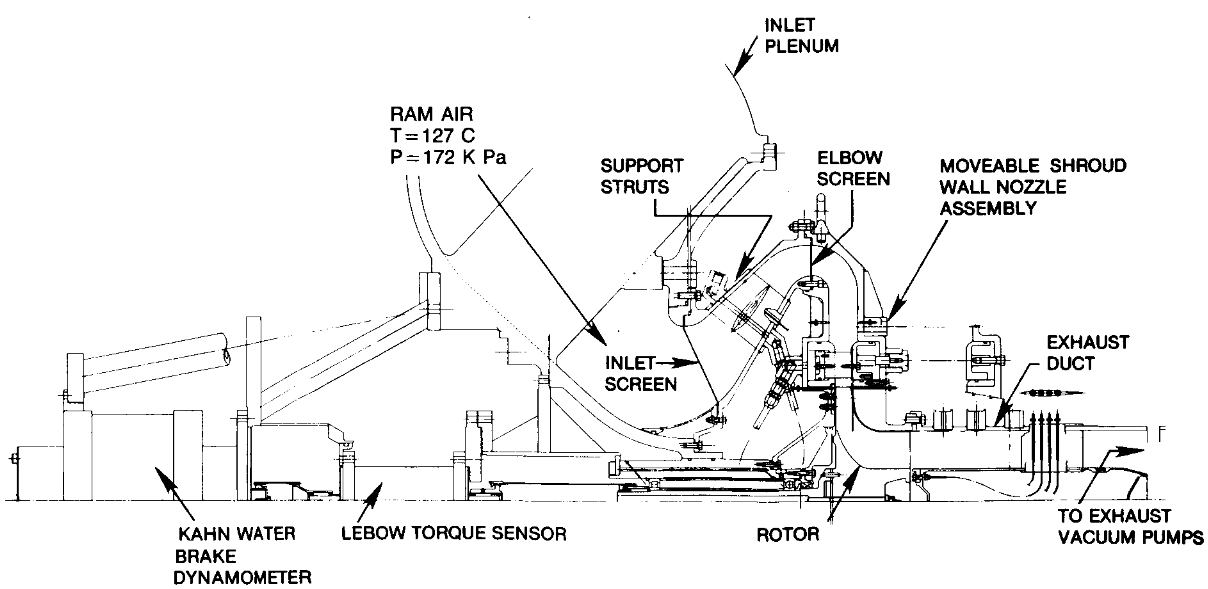

FIGURE 8. - TURBINE TEST RIG CROSS SECTION.

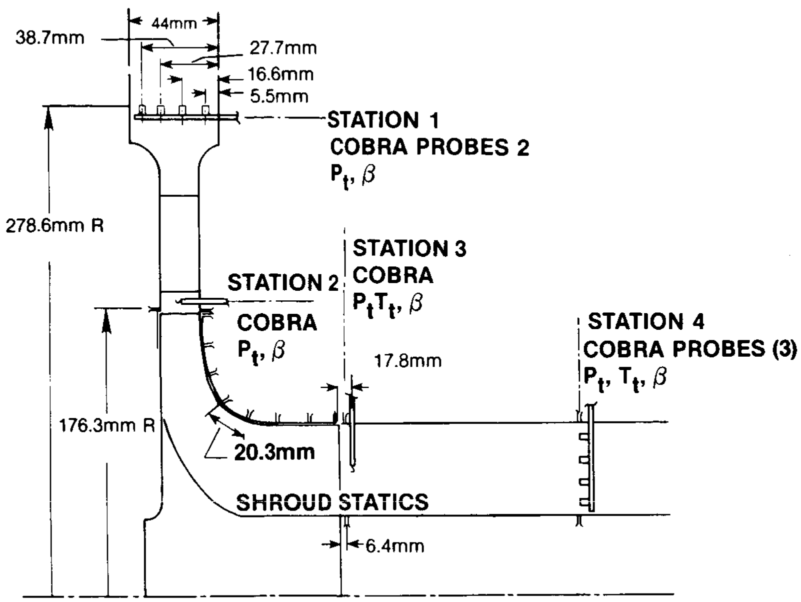

FIGURE 9. - TURBINE INSTRUMENTATION.

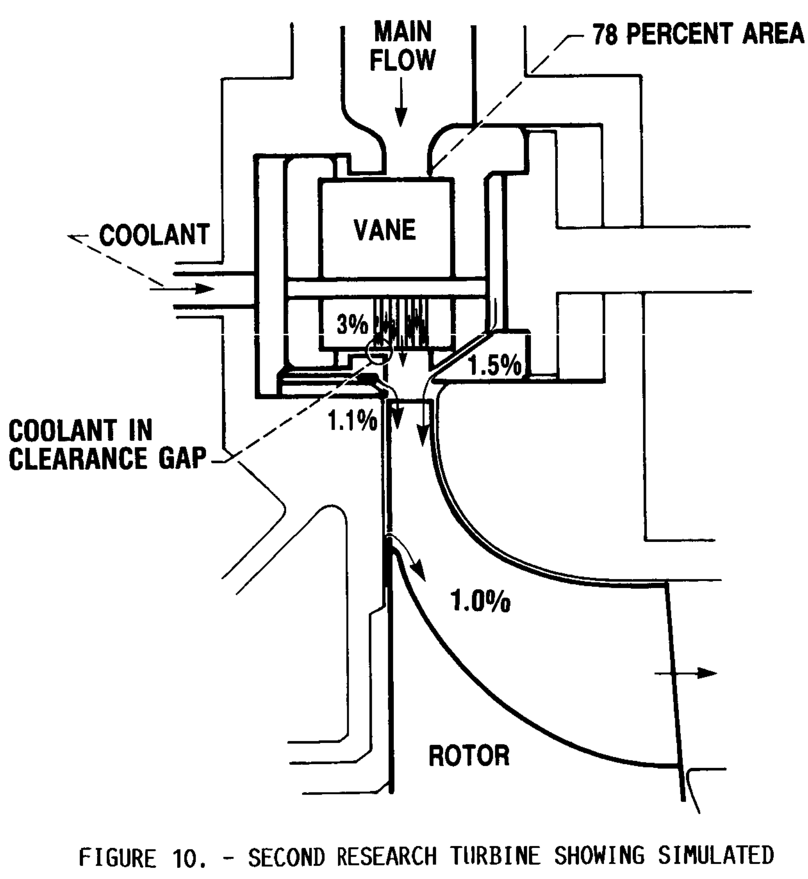

FIGURE 10. - SECOND RESEARCH TURBINE SHOWING SIMULATED COOLANT FLOWS.

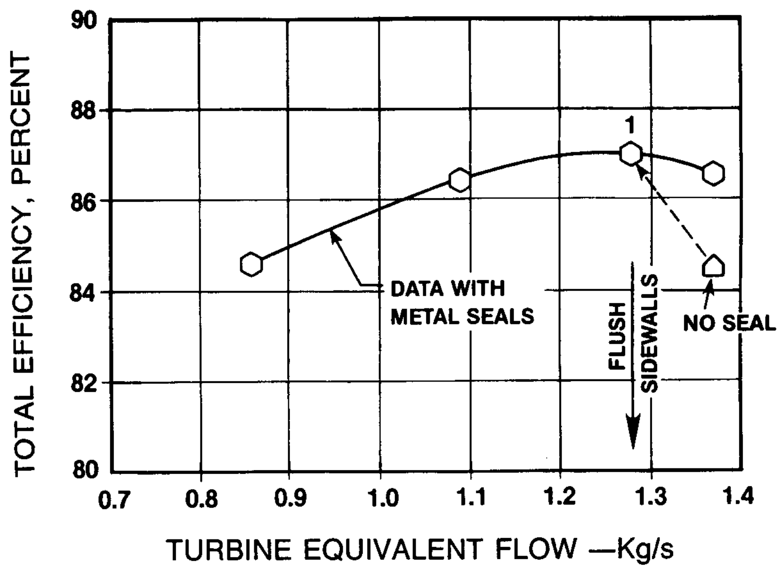

FIGURE 11. - NOZZLE LEAKAGE EFFECT ON STAGE PERFORMANCE OF FIRST TURBINE.

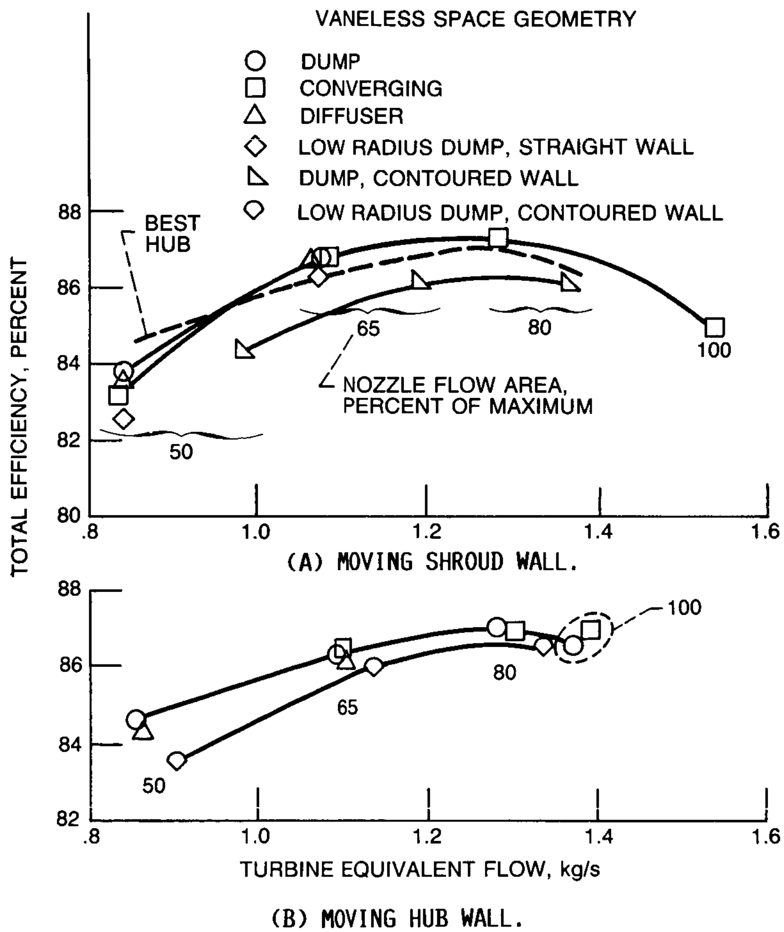

FIGURE 12. - OVERALL PERFORMANCE OF FIRST RESEARCH TURBINE DESIGN SPEED AND PRESSURE RATIO.

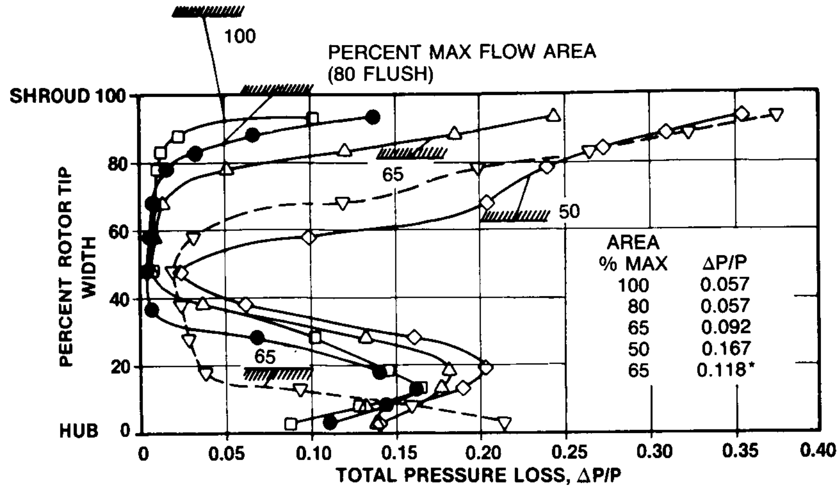

(A) TOTAL PRESSURE LOSS.

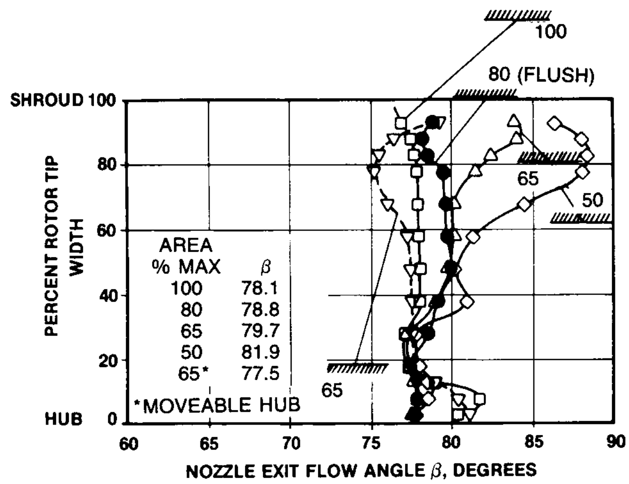

(B) FLOW ANGLE.

FIGURE 13. - NOZZLE EXIT SURVEY OF FIRST TURBINE.

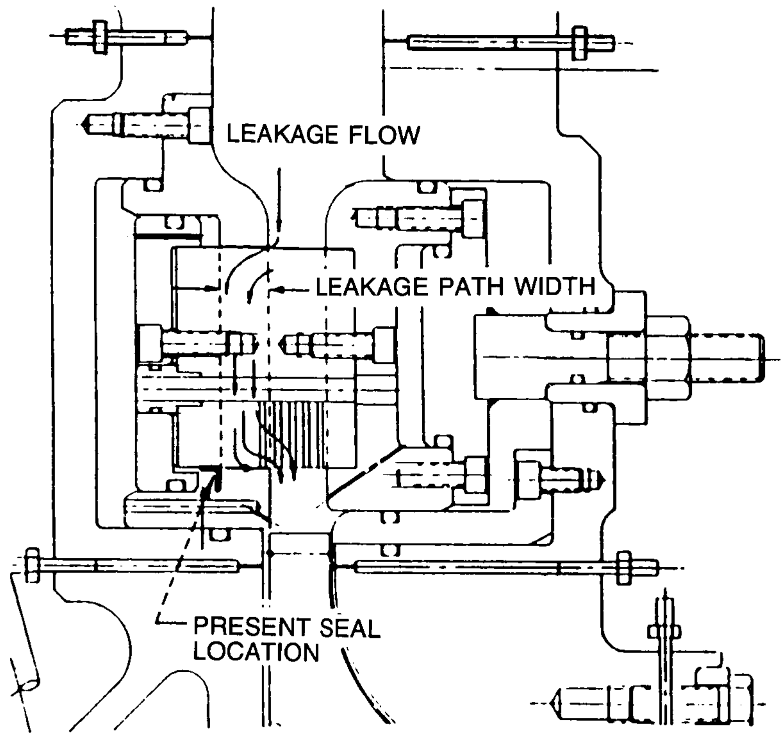

(A) TEST CONFIGURATION (TURBINES 1 & 2).

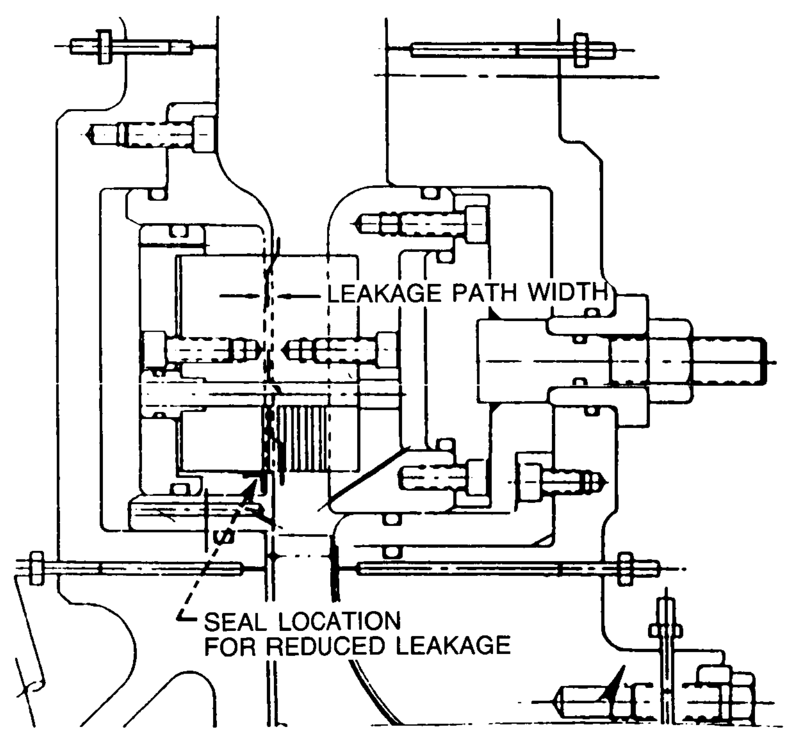

(B) CONCEPTUAL REDESIGN.

FIGURE 14. - RELOCATION OF NOZZLE SEALS TO REDUCE SIDEWALL LEAKAGE.

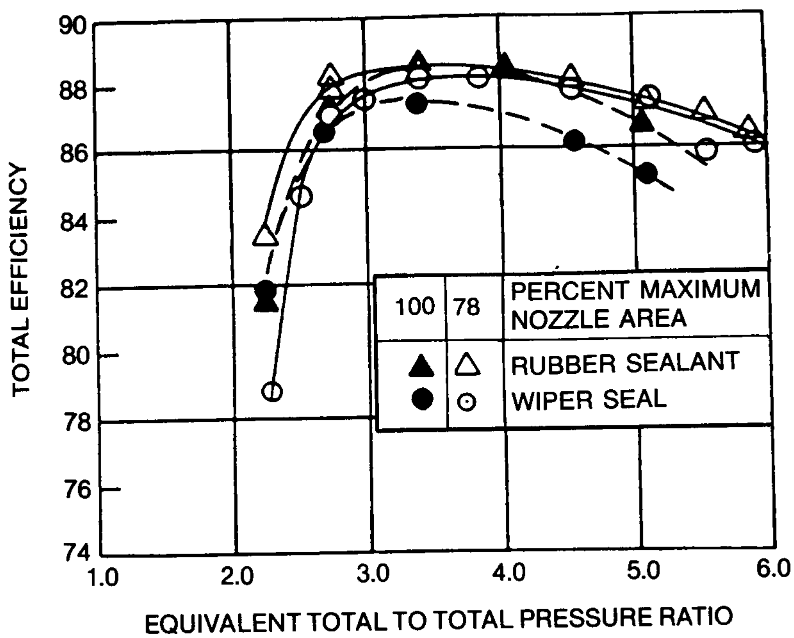

FIGURE 15. - EFFECT OF NOZZLE SEALS ON PERFORMANCE OF SECOND RESEARCH TURBINE AT DESIGN SPEED.

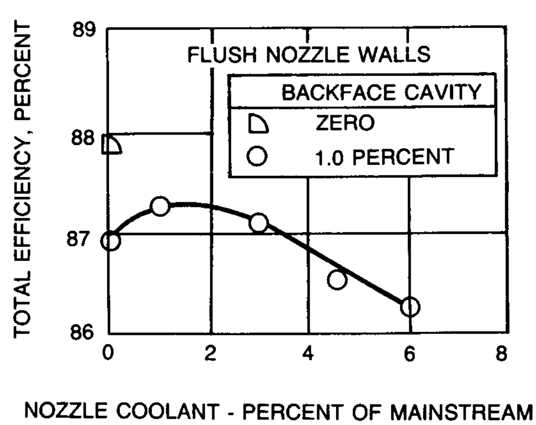

FIGURE 16. - EFFECT OF NOZZLE COOLANT ON TURBINE EFFICIENCY. DESIGN SPEED AND PRESSURE RATIO.

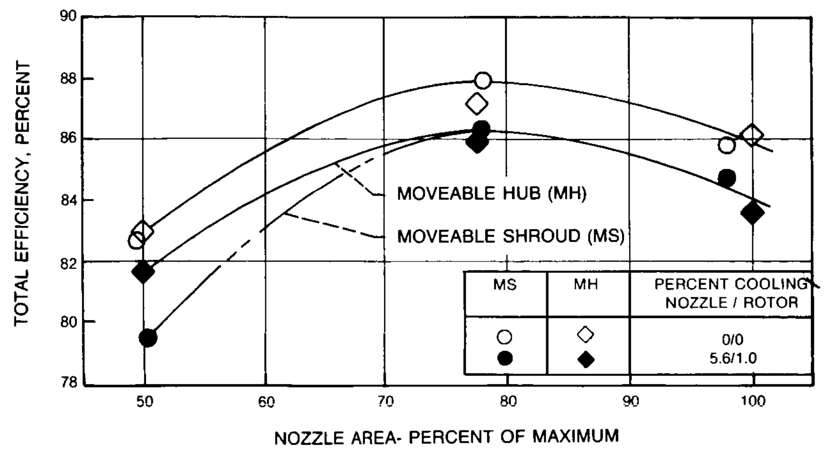

FIGURE 17. - SECOND TURBINE PERFORMANCE AT DESIGN SPEED AND PRESSURE RATIO.

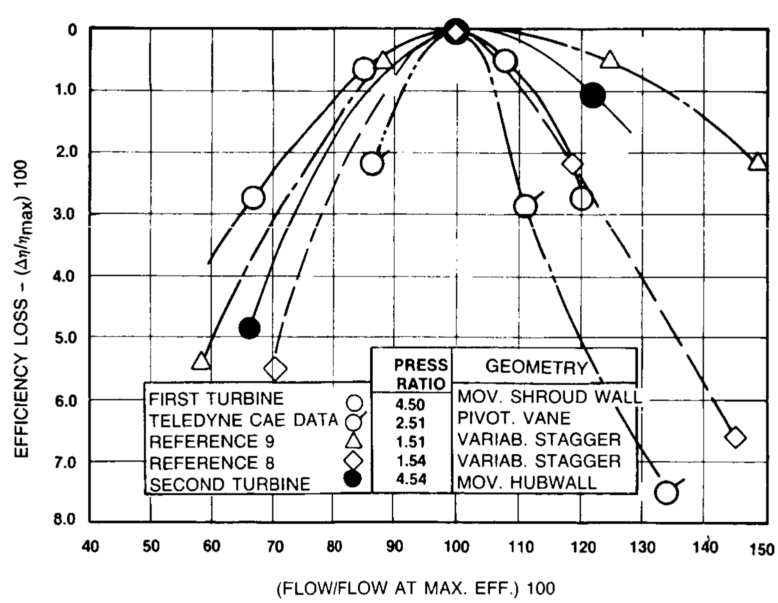

FIGURE 18. - COMPARISON OF MOVEABLE SIDEWALL AND PIVOTING VANE TURBINE PERFORMANCE.

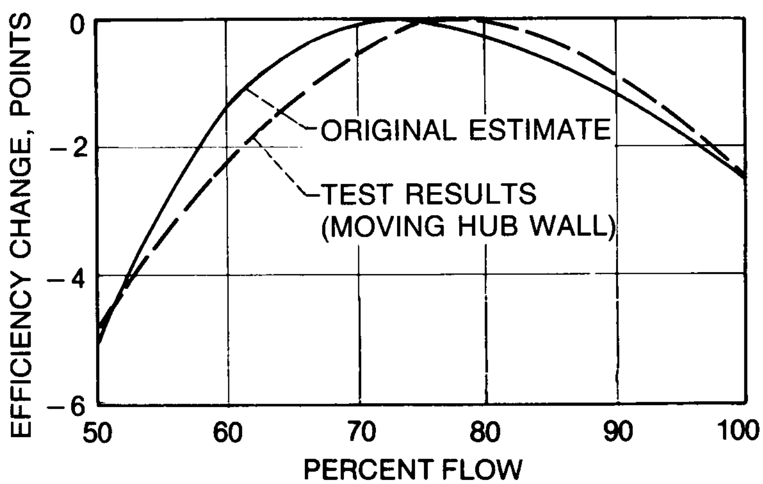

FIGURE 19. - COMPARISON OF ESTIMATED AND MEASURED CHANGE IN TURBINE EFFICIENCY WITH FLOW.

1. Report No.	2. Government Accession No.	3. Recipient's Catalog No.
NASA TM-88963		

4. Title and Subtitle	5. Report Date
Experimental Evaluation of a Translating Nozzle Sidewall Radial Turbine	
	6. Performing Organization Code 535-05-01
7. Author(s) Richard J. Roelke and Casimir Rogo	8. Performing Organization Report No. E-3419
	10. Work Unit No.
9. Performing Organization Name and Address National Aeronautics and Space Administration Lewis Research Center Cleveland, Ohio 44135	11. Contract or Grant No.
	13. Type of Report and Period Covered Technical Memorandum
12. Sponsoring Agency Name and Address National Aeronautics and Space Administration Washington, D.C. 20546	14. Sponsoring Agency Code

15. Supplementary Notes

Prepared for the 69th Symposium of the AGARD Propulsion and Energetics Panel on Technology for Advanced Aero Engine Components, Paris, France, May 4-8, 1987. Richard J. Roelke, NASA Lewis Research Center; Casimir Rogo, Teledyne CAE, 1330 Laskey Road, Toledo, Ohio 43612.

16. Abstract

Studies have shown that reduced specific fuel consumption of rotorcraft engines can be achieved with a variable capacity engine. A key component in such an engine is a high-work, high-temperature variable geometry gas generator turbine. An optimization study indicated that a radial turbine with a translating nozzle sidewall could produce high efficiency over a wide range of engine flows but substantiating data were not available. An experimental program with Teledyne CAE, Toledo, Ohio was undertaken to evaluate the moving sidewall concept. A variety of translating nozzle sidewall turbine configurations were evaluated. The effects of nozzle leakage and coolant flows were also investigated. Testing was done in warm air (121 °C). This paper summarizes the results of the contractual program.

17. Key Words (Suggested by Author(s))	18. Distribution Statement
Radial turbines Variable geometry Small engines	Unclassified - unlimited STAR Category 07

19. Security Classif. (of this report)	20. Security Classif. (of this page)	21. No. of pages	22. Price*
Unclassified	Unclassified	21	A02

*For sale by the National Technical Information Service, Springfield, Virginia 22161